THE VIRTUAL POTENTIAL FIELD METHOD AS A TOOL FOR FORMATION GUIDANCE OF AUV-S

Matko Barisic, Zoran Vukic and Nikola Miskovic
Laboratory for Underwater Systems and Technologies
University of Zagreb, Faculty of Electrical Engineering and Computing,
Unska 3
HR-10000 Zagreb, Croatia
email: {matko.barisic, zoran.vukic, nikola.miskovic}@fer.hr

ABSTRACT
This paper deals with the modifications of a kinematics-based trajectory planner for an AUV, assuring cruising in formation. Analysis is performed by means of MATLAB simulation. The method presented in authors' previous work [1, 2, 3] is redesigned, with an algorithm assigning virtual waypoints / virtual leaders for an AUV to follow in order to cruise in formation with other AUVs added.

KEY WORDS
Autonomous mobile robots, Trajectory planning, Gradients, Obstacle avoidance, Co-ordination

1 Introduction

The exploration of the immense area of the Earth's oceans will likely require the coordinated utilization of fleets of autonomous underwater robots. In order for such a paradigm to allow for efficient, correct and precise exploration of the ocean, the AUVs included in the fleet will have to possess the capability to cruise in extensive, scalable formations, and collaborate in navigation, sample collection and physical measurement of varied physical and chemical quantities. Notwithstanding problems unique to coordinated control of a swarm of robotic agents, navigation, command & control of a single AUV are in themselves problems requiring dedicated and prolonged research efforts. However, in these fields results guaranteeing the usability of a single, large, expensive system have been obtained by various research groups (AutoSub, etc.).

The coordinated control of a formation of AUVs, however, remains a research topic of utmost complexity and attractiveness for fundamental advances in the state of the robotic science. The authors have in their previous work [1, 2, 3] developed, in line with current research ongoing in virtual potentials methods (cf. [4]), a framework based on algebraic methods, [5, 6, 7], with several key advantages:

1. Intuitiveness, leading to the readability (and consequentially, easy extendibility and scalability) of implemented code. Young researchers and newcomers to the field have a steep learning curve and are able to contribute relatively easily.

2. Trivial proof of BIBO stability. The shape of the potential distribution functions of the features of the trajectory planning problem (robotic agent, obstacle, waypoint) can be selected so that the resulting physical system is at the very least conservative. Modifications have been undertaken in [1] so that the system is indeed dissipative and therefore asymptotically stable, with a Lyapunov-like proof.

3. The method operates on thrust vectors, allowing for cross-platform portability since thruster allocation can be programmed separately to conform to certain actuator configurations.

4. A good number (not too great, not too small) of method-independent parameters that allow for:

   - Further automated decision-making above and beyond the problem of trajectory planning, in the form of online setting or adaptation of these parameters (e.g. automated decision-making related to the risk represented by cruising closer to a certain obstacle by lowering its repulsiveness).
   - Easy formulation of various optimization problems of engineering merit when considering a certain AUV craft that the algorithm is to be implemented in.

5. Cross-layer-design features. A number of important behavioral paradigms:

   - obstacle avoidance,
   - top-speed cruising through unobstructed water,
   - predictive circumnavigation of an obstacle allowing for the minimization of actuator energy (especially important in cruise-type, torpedo-hulled AUVs [9, 10] where heading changes are effected through a rudder that can come under a lot of stress in steep and fast maneuvers),
   - formation assembly,
   - partial formation break-up for purposes of obstacle circumnavigation,
   - formation reassembly in unobstructed water etc.

Are all achieved without recourse to separate procedures and programmatic modules.

However, the developed framework exhibited a lack of asymptotical stability of the formation. The AUVs would all converge to the general vicinity of the waypoint, but an "all stop" command was never realized. Finite and non-vanishing jitter was introduced as a side-effect of the chaotic perturbations of local minima. Within every AUV of the formation, a collection of local minima was continually being "*dragged*" by every other observed AUV in the same formation, influencing in turn its own manoeuvring. In this way a nonlinear and non-deterministic feedback effect was inadvertently achieved.

This shortcoming was resolved with the redesign proposed in this paper in Section 3. Before approaching the redesign, Section 2 revisits the original design of the virtual potential method trajectory planner. Section 4 displays the simulated performance of the redesigned method. Section 5 concludes the paper.

2 The Virtual Potentials Method

The virtual potential based trajectory planner previously developed by the authors in [1, 2, 3], ensures proper trajectory planning with respect to obstacles within the N-dimensional mission space of an AUV. The influence is in general a "force-like" vectored quantity depending in modulus and argument on the gradient of a scalar field. The scalar field is calculated in the sensor space as a summation of values of virtual potential distribution functions, or decentralized control functions, attributed to each and every observed obstacle. Mathematically, the influence of n obstacles on the AUV trajectory is represented by a summation $E_s(\vec{p}) = \sum_{i=1}^{n} f_s^{(i)}$, where each $f_{obs}^{(i)}(\cdot), i = 1 \dots N$ is given by:

$$f_{obs}^{(i)}(\vec{x}) = \exp\left\{A_s^{+(i)} / r^{(i)}\left[\vec{x}_{obs}^{(i)}\right](\vec{x})\right\} \qquad (1)$$

Where:
- $\vec{x}$ is the vector of point coordinates in the mission space, $\vec{x} \in \mathbb{R}^N$,
- $r^{(i)}\left[\vec{x}_{obs}^{(i)}\right](\mathbb{R}^N) \in \mathbb{R}_0^+$ is the function that returns the distance between the AUV's location and the i-th obstacle ($r^{(i)}$-s is indexed by i, since it can vary depending on the geometric shape of the obstacle $obs^{(i)}$), parameterized by a representative point of the i-th obstacle, $\vec{x}_{obs}^{(i)} \in \mathbb{R}^N$ (geometric barycenter or some other typical point of the obstacle, e.g. a polygon vertex),
- $A_s^{+(i)} \in \mathbb{R}_0^+$ is the repulsion amplification attributed to the i-th obstacle.

In [3], a modification was implemented in order to reformulate the problem to avoid the appearance of local extremals, based on the idea of *rotor potentials*. In the modification, the vector influencing the trajectory planning is formed from the addition of the previously explained gradient vector and a vector perpendicular to the line along the shortest distance between the obstacle and the AUV, whose magnitude varies with that distance. The mathematics, recapitulated from [3], is the following:

$$\begin{aligned}
E_s(\vec{x}) &\rightarrow E(\vec{x}) \\
\therefore E(\vec{x}) &\doteq E_s(\vec{x}) + E_r(\vec{x}) \\
&= \sum_{i=1}^{n} f_s^{(i)}(\vec{x}) + \sum_{i=1}^{n} f_r^{(i)}[\vec{x}_r](\vec{x}) \\
&= \sum_{i=1}^{n} \left\{ f_s^{(i)}(\vec{x}) + f_r^{(i)}[\vec{x}_r](\vec{x}) \right\} \\
\therefore f_{obj}[\vec{x}_r] &\doteq f_s + f_r[\vec{x}_r] \qquad (2)
\end{aligned}$$

Where:
- E_s is the stator part of the scalar field E,
- E_r is the rotor part of the scalar field E,
- $f_s^{(i)}$ is the stator potential distribution function of an i-th feature or obstacle,
- $f_r^{(i)}[\vec{x}_r]$ is the rotor potential distribution function of an i-th feature or obstacle *with respect to a predetermined reference point in the mission space*, $\vec{x}_r$,
- $f_{obj}[\vec{x}_r](\cdot)$, is the aggregate potential distribution function, which has now needs to additionally be parameterized by $\vec{x}_r$, since rotor potentials are calculated w.r.t. a reference point in the mission space, being dependent on the geometrical relationship between the representative point of the object to which f_{obj} is attached, $\vec{x}_{obs}$, and the said reference point.

More precisely, as detailed in [3] and following the form in (2), the potential distribution functions of obstacles are:

$$f_{obj}(\vec{x}) = f_s(\vec{x}) + f_r\left[A_r^+, \vec{x}_{obs}, \vec{p}\right](\vec{p}) \qquad (3)$$

Where:
- $f_r\left[A_r^+, \vec{x}_{obs}, \vec{p} \in \mathbb{R}^N\right]\left(\mathbb{R}^N\right)$ is a rotor potential function parameterized by A_r^+, $\vec{x}_{obs}$ and $\vec{p}$, the coordinate vector of the AUV under observation,
- A_r^+ is the rotor amplification,
- $\vec{p}$, used identically instead of $\vec{x}_r$ is the coordinated vector of the AUV under observation.

The identity $\vec{x}_r \equiv \vec{p}_{AUV}$ shall always be assumed unless explicitly stated otherwise. This allows for some shortening of notation by omission of $\vec{x}_r$ in the parameter list for f_{obj}-type potential distribution functions. Moreover, this has the direct consequence further (also discussed in more detail in [3]):

$$\begin{aligned}
f_r(\vec{p}) &\equiv 0 \\
&\Rightarrow \\
f_{obj}(\vec{p}) &\equiv f_s(\vec{p})
\end{aligned}$$

The gradient of the scalar field $E(\vec{p}) = \sum_{N}^{i=1} f_{obs}^{(i)}$ is numerically approximated by the sampling of the scalar field E at the AUV's position, $\vec{p}$, and an m-tuple of sampling points spaced equidistantly along the circle of radius

r_ϵ around $\vec{p}$, at angular increments of $2\pi/m$:

$$\begin{aligned}\mathcal{E} &= \left\{\epsilon^{(i)}(k)\right\} \\ \epsilon^{(i)}(k) &= \vec{p}(k) + r_\epsilon \cdot [\cos(2\pi i/m) \;\; \sin(2\pi i/m)]^{\mathrm{T}}\end{aligned}$$

The gradient, equal to the non-friction component of the controlling force, $\vec{F}_{nf}(k)$, is then approximated as follows:

$$\begin{aligned}\left|\vec{F}_{nf}(k)\right| &= \max_i \left[E\left(\vec{p}(k)\right) - E\left(\vec{\epsilon}^{(i)}(k)\right)\right] \\ \angle\vec{F}_{nf}(k) &= \arg\max_i \left[E\left(\vec{p}(k)\right) - E\left(\vec{\epsilon}^{(i)}(k)\right)\right] \\ \vec{F}(k) &= \vec{F}_{nf}(k) + \mu \cdot \vec{v}(k-1) \quad (4) \\ \overline{\vec{F}}(k) &= \vec{F}(k)/\left|\vec{F}(k)\right| \cdot \inf\left(\left|\vec{F}(k)\right|, F_{max}\right) \quad (5)\end{aligned}$$

Where:
- $\vec{F}_{nf}(k)$ is the no-friction controlling force term (cf. [1, 2]),
- $\vec{F}(k)$ is the controlling force with virtual viscose friction taken into account (cf. [1, 2]), which when bounded on the upper side by F_{max} is denoted $\overline{\vec{F}}(k)$,
- $\vec{v}(k-1)$ is the actual measured velocity vector of the AUV at time $k-1$.

If the actuator control subsystem of a particular AUV has predefined points of entry, rather than being able to accept a controlling force as a feed, the controlling force (based on the completely holonomic model of the kinematics) can be decomposed into set-point feeds appropriate for parallel structure PI-D controllers for the surge speed (the linear acceleration command, the commanded surge speed and the integral command) and heading rate (the angular acceleration command, the commanded heading change rate and the commanded heading), $\{(a_c, v_c, I_{surge}), (\alpha_c, \omega_c, \phi_c)\}$:

$$\begin{aligned}\vec{v}_c(k) &= T/2 \cdot \left(\vec{F}(k-1) + \vec{F}(k)\right) + \vec{v}(k-1) \quad (6) \\ \overline{\vec{v}_c}(k) &= \vec{v}_c(k)/\left|\vec{v}_c(k)\right| \cdot \inf\left(\left|\vec{v}_c(k)\right|, v_{max}\right) \quad (7) \\ \overline{\vec{v}_c}(k) &= \langle\overline{\vec{v}_c}(k), \hat{\mathbf{e}}_1\rangle \cdot \hat{\mathbf{e}}_1 + \langle\overline{\vec{v}_c}(k), \hat{\mathbf{e}}_2\rangle \cdot \hat{\mathbf{e}}_2 \quad (8) \\ \hat{\mathbf{e}}_1 &= \vec{v}_c(k-1)/\left|\vec{v}_c(k-1)\right| \quad (9) \\ \hat{\mathbf{e}}_2 &= \begin{bmatrix} 0 & 1 \\ -1 & 0 \end{bmatrix} \cdot \hat{\mathbf{e}}_1 \quad (10) \\ v_c(k) &= \langle\vec{v}_c(k), \hat{\mathbf{e}}_1\rangle\end{aligned}$$

Where:
- $\vec{v}(\cdot)$ is the *actual* speed vector in the Earth-fixed frame of reference at whichever time instant (k, $k-1$, etc.),
- $\vec{v}_c(\cdot)$ is the speed command *vector* in the Earth-fixed frame of reference at whichever time instant (k, $k-1$ etc.), which when bound on the upper side is denoted $\overline{\vec{v}_c}(k)$,
- $v_c(\cdot)$ is the surge speed command at whichever time instant (k, $k-1$ etc.),
- $(\hat{\mathbf{e}}_1, \hat{\mathbf{e}}_2)$ are an orthonormal basis in the AUV's body-fixed frame of reference at $k-1$, expressed in the Earth-fixed frame of reference,
- $\langle\cdot,\cdot\rangle$ is the scalar product of two vectors, $\langle\vec{a}, \vec{b}\rangle = |\vec{a}| \cdot \left|\vec{b}\right| \cdot \cos\angle\left(\vec{a}, \vec{b}\right)$.

$$a_c = \left|\vec{F}(k)\right|$$

Where:
- $a_c(k)$ is the derivative channel (acceleration) command for the parallel surge speed PI-D controller at time k.

$$\begin{aligned}\phi(k-1) &= \text{atan2}\left(\vec{v}(k-1)\right) \\ \phi_c(k) &= \text{atan2}\left(\vec{v}_c(k)\right)\end{aligned}$$

Where:
- $\phi(k-1)$ is the *actual* heading at time $k-1$,
- $\phi_c(k)$ is the heading command at time k,
- $\mathrm{atan2}(\cdot)$ is the four-quadrant arc-tangent (in an Earth-fixed frame of reference).

$$I_{surge} = |\vec{p}(k) - \vec{p}_c(k)|$$

Where:
- $\vec{p}(k)$ is the *actual* position vector of the AUV,
- $\vec{p}_c(k)$ is the commanded or idealized expected position of a *double-integrator* dynamic model of the AUV.

$$\begin{aligned}\omega(k-1) &= \left[\phi(k-1) - \phi(k-2)\right]/T \\ \omega_c(k) &= \left[\phi_c(k) - \phi(k-1)\right]/T\end{aligned}$$

Where:
- $\omega(k-1)$ is the actual heading change rate at time $k-1$,
- $\omega_c(k)$ is the heading change rate command at time k.

$$\begin{aligned}r\left(k-1|k-1\right) &= \omega(k-1)/v(k-1) \\ r\left(k|k-1\right) &= \omega_c(k)/v_c(k)\end{aligned}$$

Where:
- $v(k-1)$ is the actual measured surge speed of the AUV at time $k-1$,
- $v_c(k)$ is the surge speed command of the AUV at time k,
- $r\left(k|k-1\right)$ is the turning radius of the AUV at time k with true navigation data last sampled in time instance $k-1$,
- $r\left(k-1|k-1\right)$ is the turn radius of the AUV at time $k-1$ with true navigation data at that time instance known.

$$\begin{aligned}\alpha_c(k) &= \Big\{r(k) \cdot a_c(k) - \ldots \\ &\qquad v_c(k) \cdot \left[r\left(k|k-1\right) - r\left(k-1|k-1\right)\right]/T\Big\}/\ldots \\ &\qquad r^2\left(k|k-1\right)\end{aligned}$$

Where:
- $\alpha_c(k)$ is the derivative channel of the parallel heading rate PI-D controller at time k.

3 The Redesign of the Method

3.1 Ensuring Heading-Rate Reserve When Maneuvering Near Maximum Forward Speed

Consider the repercussions of (7) when an AUV is approaching an obstacle after a prolonged period of acceleration through unobstructed water. If the obstacle is situated mid-way between the initial point and the waypoint that the AUV is trying to reach, the slope of the inverted bell-shaped curve of the waypoint's potential distribution function (cf. [2]) will be steepest. Therefore, it is likely that the *controlling force* given by (5) will be equal to F_{max}. If the AUV had been accelerating without obstruction for some time, its forward speed, v will be identically equal to v_c, which will be v_{max}.

In this scenario, depending on the configuration of the AUV's thrusters, it might not be possible for AUV to start to circumnavigate the obstacle while ideally still some distance away from the obstacle. Rather, the AUV will enter the region wherein the repulsive influence of the obstacle will cause it to slow down significantly, only to accelerate after having circumnavigated it. In essence this is a type of *wind-up* of the *controlling force* significantly degrading the parsimony of AUV's energy expenditure and balance in obstacle-avoidance maneuvers.

To arrive at a solution to this problem, redefine the bound operation in (5) by first decomposing $\vec{F}(k)$ as defined by (4) into components parallel and perpendicular to the current direction of travel of AUV, given by the argument of the true velocity vector of the AUV at time instant $k-1$, $\vec{v}(k-1)$, making use of the orthonormal base defined in (9, 10), and decomposing the *controlling force* in a similar manner to that in which the command velocity vector, $\vec{v}_c(k)$ was decomposed in (8):

$$\begin{aligned}\vec{F}(k) &= \langle\vec{F}(k),\hat{\mathbf{e}}_1\rangle\cdot\hat{\mathbf{e}}_1+\langle\vec{F}(k),\hat{\mathbf{e}}_2\rangle\cdot\hat{\mathbf{e}}_2\\ \vec{F}(k) &= F_{\parallel}(k)\cdot\hat{\mathbf{e}}_1+F_{\perp}(k)\cdot\hat{\mathbf{e}}_2\end{aligned}$$

Where:
- $F_{\parallel}(k)$ is the component of $\vec{F}(k)$ parallel to the current direction of travel of the AUV, given by $\angle(\vec{v}(k))$,
- $F_{\perp}(k)$ is the component of $\vec{F}(k)$ perpendicular to the current direction of travel of the AUV.

If the parallel component is negative (meaning speed should be commanded to decrease), then the bounding procedure is executed as follows:

1. If necessary, bound the parallel component to satisfy the maximum force constraint:

$$\overline{F}_{\parallel}(k) = -\inf\left(F_{max},\left|F_{\parallel}(k)\right|\right)$$

2. If necessary, bound the perpendicular component to satisfy the maximum force constraint:

$$\overline{F}_{\perp}(k) = \operatorname{sgn}\left(F_{\perp}(k)\right)\cdot\inf\left(\left|F_{\perp}(k)\right|,\sqrt{F_{max}^2-\overline{F}_{\parallel}^2(k)}\right)$$

Otherwise (the parallel component is nonnegative), the order of the bounding operations is reversed:

1. If necessary, bound the perpendicular component to satisfy the maximum force constraint:

$$\overline{F}_{\perp}(k) = \operatorname{sgn}\left(F_{\perp}(k)\right)\cdot\inf\left(F_{max},\left|F_{\perp}(k)\right|\right)$$

2. If necessary, bound the parallel component to satisfy the maximum force constraint:

$$\overline{F}_{\parallel}(k) = \inf\left(\left|F_{\parallel}(k)\right|,\sqrt{F_{max}^2-\overline{F}_{\perp}^2(k)}\right)$$

The bounding procedure for the commanded velocity vector is redefined in exactly the same procedure, i.e. if $\vec{v}_{\parallel c}(k)=\langle\vec{v}_c(k),\hat{\mathbf{e}}_1\rangle$ in (8) is negative: If the parallel component is negative (meaning speed should be commanded to decrease), then the bounding procedure is executed as follows:

1. If necessary, bound the parallel component to satisfy the maximum velocity constraint:

$$\overline{v}_{\parallel c}(k) = -\inf\left(v_{max},\left|v_{\parallel c}(k)\right|\right)$$

2. If necessary, bound the perpendicular component to satisfy the maximum velocity constraint:

$$\overline{v}_{\perp c}(k) = \operatorname{sgn}\left(v_{\perp c}(k)\right)\cdot\inf\left(\left|v_{\perp c}(k)\right|,\sqrt{v_{max}^2-\overline{v}_{\parallel c}^2(k)}\right)$$

Otherwise:

1. If necessary, bound the perpendicular component to satisfy the maximum velocity constraint:

$$\overline{v}_{\perp c}(k) = \operatorname{sgn}\left(v_{\perp c}(k)\right)\cdot\inf\left(v_{max},\left|v_{\perp c}(k)\right|\right)$$

2. If necessary, bound the parallel component to satisfy the maximum velocity constraint:

$$\overline{v}_{\parallel c}(k) = \inf\left(\left|v_{\parallel c}(k)\right|,\sqrt{v_{max}^2-\overline{v}_{\perp c}^2(k)}\right)$$

In this way, regardless of the acceleration along the current course, $\phi(k)$, the AUV's trajectory will always be planned so as to start circumnavigating obstacles in front of it at the earliest possible time.

3.2 Assignation of Formation-Based Virtual Leaders

In previous work, especially [2, 3], the formation of AUVs cooperating in a group was achieved asymptotically by having other AUVs sensed by an AUV planning the trajectory represented as a following type of potential distribution function:

$$\begin{aligned}f_{ag}(\vec{x}) &= f_{circ}\left[\vec{x}_{ag}\right](\vec{p})\\ &\quad+\sum_{q}^{i=1}f_{gp}\left[\vec{\nu}_{ag}^{(i)}\right](\vec{x})\end{aligned}\qquad(11)$$

Where:
- $f_{ag}(\mathbb{R}^N)$ is the potential distribution function attached to an agent – another AUV navigating in formation with the AUV under observation, located at $\vec{x}_{ag}$
- $f_{circ}\left[\vec{x}_{ag}\right](\mathbb{R}^N)$ is the potential distribution function of the circular type (cf. [2, 3]), the circle being centered on $\vec{x}_{ag}$, coordinates of the agent,
- $f_{gp}\left[\vec{\nu}_{ag}^{(i)}\right](\mathbb{R}^N)$ are the $q \in \mathbb{N}$ potential distribution functions of the Gaussian or goal-point type (cf. [2, 3]), given in (12), each one centered on the corresponding $\vec{\nu}_{ag}^{(i)}$, the coordinate vector of the formation-nodes surrounding the agent, and defined by:

$$\vec{\nu}_{ag}^{(i)} = \vec{x}_{ag} + \lambda \left[\cos 2\pi i/q \ \sin 2\pi i/q\right]^{\mathrm{T}}$$

Where:
- $\lambda \in \mathbb{R}_0^+$ is the length of the formation lattice, i.e. the ideal distance at which AUVs in formation should be away from each other when cruising in perfect formation,
- q is the *formation descriptor*, one of the three possible numbers of vertices of regular polygons which completely tile the 2D plane (equilateral triangle, square, regular hexagon).

$$f_{gp}\left[\vec{\nu}_{ag}^{(i)}\right](\vec{x}) = -A^- \cdot \exp\left(-\|\vec{x} - \vec{\nu}_{ag}^{(i)}\|^2 / 2\sigma^2\right) \quad (12)$$

Where:
- $A^- \in \mathbb{R}_0^+$ is the attraction coefficient,
- $\vec{x} \in \mathbb{R}^N$ is the point in the mission space at which potential is being evaluated,
- $\sigma \in \mathbb{R}_0^+$ is the coefficient tuning the "spread" of the Gaussian potential distribution function (cf. [2, 3]) of every formation node, identically equal to $\lambda/3$, so that the "inverse bell" of the Gaussian potential distribution functions $f_{gp}^{(1\ldots q)}$ each contributing to the composite agent's potential distribution function f_{ag} by each of the q formation nodes around it *"taper away"* at the position of the agent itself.

The example of a potential described by (11), for $q = 3$, is given by figure 1.

However, in a formation of more than 2 AUVs, this leads to chaotic behavior [10] which is extremely difficult to *regularize*. Moreover, techniques that would be able to regularize or attenuate this chaotic behavior would break the *cross-layer design* paradigm and thereby introduce elements of non-scalable and non-extendible design into this framework.

In contrast to such solutions, the chaotical interaction of local minima in figure 1, attached to each AUV in a formation, and moving with their complex and mutually influenced motion, can be avoided by introducing a layer that for each AUV planning the trajectory, introduces only *one* local minimum in the form of a virtual leader.

The typical non-ideal and non-stationary situation in this formation-maintaining problem is displayed in figure 2.

An alternative algorithm, uniquely placing one local minimum or one virtual waypoint, is developed in table 1.

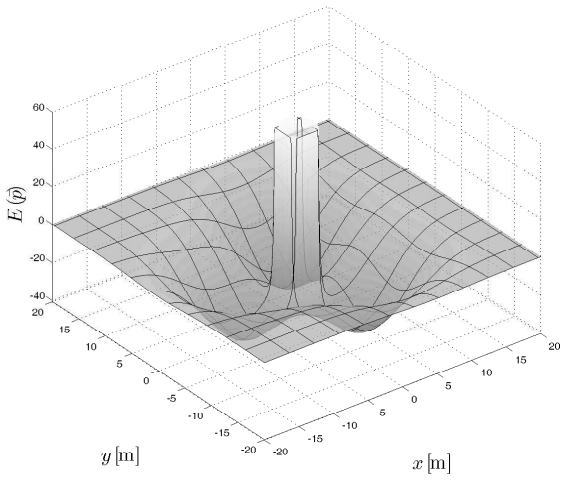

Figure 1. The potential distribution function for an agent, with $n = 3$, in authors' previous work [1, 2, 3]

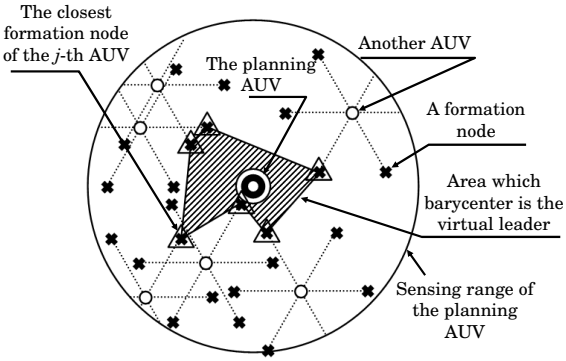

Figure 2. A typical situation with multiple other AUVs near the AUV planning the trajectory.

Table 1. The virtual leader algorithm

1.	Initialize $\mathbf{VL}$ as an empty (0×0) matrix.
Loop 1	For each sensed agent i located at $\vec{x}_{ag}^{(i)}$
(L1.1)	Take the angle $\beta_i = \mathrm{atan2}\left(\vec{x}_{ag}^{(i)} - \vec{p}\right)$
(L1.2)	Quantize the angle β_i by $\pi/3$ to arrive at $k \in (1 \ldots q)$, the ordinal number of the optimally fitting node for the i-th sensed agent.
(L1.3)	Append the row $\mathbf{vl}(i) = \vec{x}_{ag}^{(i)\ \mathrm{T}} + [\lambda \cos(k\pi/3), \lambda \sin(k\pi/3)]$
End L1	
2.	Take the *column-mean* (add up rows and divide by number of rows) of $\mathbf{VL}$, $\vec{\nu} = \mathrm{colmean}(\mathbf{VL})^{\mathrm{T}}$.
3.	Place a virtual leader / virtual waypoint potential distribution function at $\vec{\nu}$.

4 Simulative Analysis

Two simulations, exploring the behavior of the algorithm in an uncluttered mission theater, and in a severely cluttered mission theater were performed.

The paths planned for each of the 4 AUVs in the unobstructed mission theater simulation are given in figure 3. The helm speed commands are given in 4.

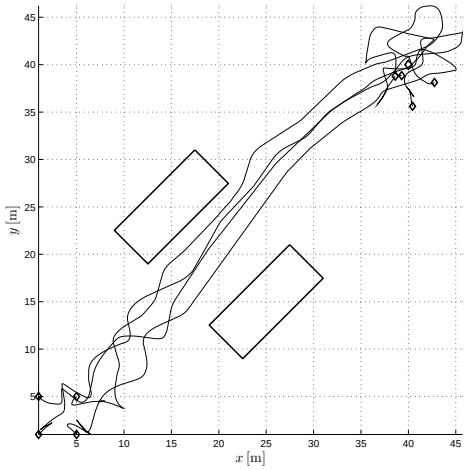

Figure 3. The paths planned for a formation of 4 AUVs in an uncluttered mission theater.

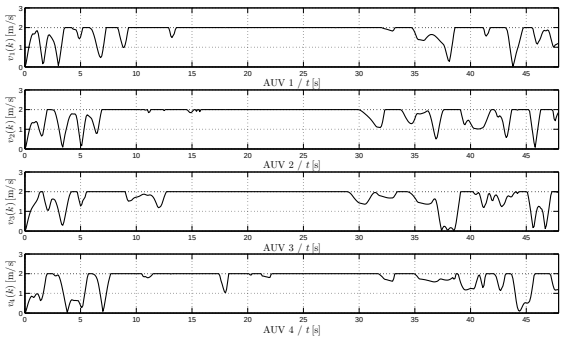

Figure 4. The helm speed commands of the 4 AUVs navigating in formation in an uncluttered mission theater.

The paths planned for each of the 4 AUVs in the severely cluttered mission theater are given in figure 5. The helm speed commands are given in 6.

5 Conclusion And Further Work

5.1 Concluding remarks

In conclusion, the framework presented in author's previous work was improved by the redesign of the method by which formation is assembled, disassembled while circumnavigating the obstacles and reassembled when once more possible. In the analysis of the simulation, performed as a *software sanity test*, it was shown that the new design methodology is robust to the level of clutter and that it can successfully reestablish the formation once AUVs have split apart in order to circumnavigate the obstacles while

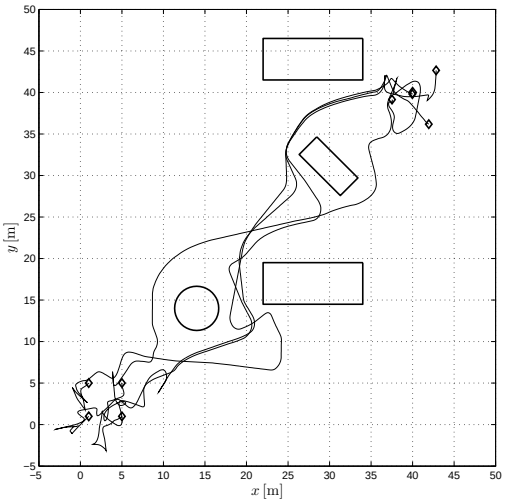

Figure 5. The paths planned for a formation of 4 AUVs in a severely cluttered mission theater.

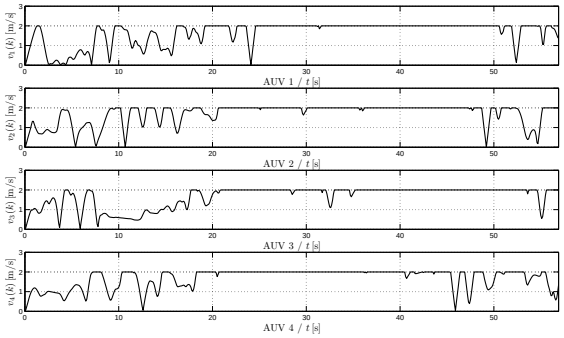

Figure 6. The helm speed commands of the 4 AUVs navigating in formation in a severely cluttered mission theater.

expending the minimum of energy on avoidance maneuvers.

Thereby, the redesigned framework acts as a middle level of an integrated and embedded intelligent control system for a formation of AUVs under development in the authors' laboratory. This framework, sitting in a hierarchical tier structure above the AUV's drive (thruster, rudder etc.) controllers, produces commands that these controller need to servo as best possible.

Towards an even higher level of abstraction, various signals incipient in normalization and bounding procedures described in authors' previous work, as well as in Subsection 3.1. can be regarded as either boolean or real signals on the basis of which certain residuals can be generated. By exploiting such a hybrid analysis of the operation of this framework, a set of boolean flags can be arrived at that monitor and encode information about the system. These can be linked to rules in an inference system, which can

serve at the highest semantic levels in order to determine categorical descriptions of the course of the mission.

5.2 Future research

Future research will be directed towards the exploration of the following topics:

1. Exploring the thruster allocation aspect of how the controlling force can best be reproduced by various thruster configurations – researching holonomy constraints, and inspecting the possible introductions of *diffeomorphism* alike to the one used in [11].

2. Estimation of stationary stochastic disturbances in the mission theater, like currents, wave motion, drift etc. by the analysis of the trends exhibited in the guidance errors (differences between actual measurement of the AUV's navigational states and the commands produced by the proposed trajectory planner).

Acknowledgements

This research was made possible through the following contributions:

1. *Professional and technological equipment* — An FP7 Capacities Project in Response to the REGPOT-2008-1 Call, ***"Strengthening the Croatian Underwater Robotics Research Potential – CURE"***.

2. *Scientific and professional secondment / internship grant* — "Unity Through Knowledge Fund", MOSES[1], Croatia.

3. *fieldwork financing* provided by the Center for Underwater Systems and Technologies, Zagreb[2].

6 References

[1] Barisic, M., Vukic, Z., and Miskovic, N., A Kinematic Virtual Potentials Trajectory Planer for AUVs *Proceedings of the 6th IFAC Symposium on Intelligent Autonomous Vehicles*, Devy, M. (ed.), CNRS Laboratoire d'Architecture et d'Analyse des Systemes, Tolouse, France, 2007, on CD.

[2] Barisic, M., Vukic, Z., and Miskovic, N. Kinematic Simulative Analysis of Virtual Potential Field Method for AUV Trajectory Planning, *Proceedings of the 15th Mediterranean Conference on Control and Automation*, Valavanis, K., and Kovacic, Z. (ed.), Athens, Greece, 2007, on CD.

[3] Barisic, M., Vukic, Z., and Omerdic, E., Introduction of Rotors to a Virtual Potentials UUV Trajectory Planner, *Proceedings of the Workshop on Navigation, Guidance and Control of Underwater Vehicles 2008*, Toal, D., and Roberts, G., Limerick, Ireland, 2008, on CD.

[4] Schwartz, H.M., and Givigi Jr., S.N., A Practical Approach to Robotic Swarms, *Proceedings of the Tenth IASTED International Conference on Control Applications*, Rabbath, C.A. (ed.), Quebec City, Quebec, Canada, 2008, on CD.

[5] Fiorelli, E. *et al.*, Multi-AUV Control and Adaptive Sampling in Monterey Bay, *Proc. of the IEEE Autonomous Underwater Vehicles 2004: Workshop on Multiple AUV Operations*, pp. 134-147.

[6] Sepulchre R., Paley D. and Leonard N. E., Graph Laplacian and Lyapunov Design of Collective Planar Motions, *Proceedings of the International Symposium on Nonlinear Theory and Its Applications*, The Institute of Electronics, Information and Communication Engineers, Tokyo, Japan, on CD.

[7] Kalantar, S., and Zimmer, U., Motion planning for small formations of autonomous vehicles navigating on gradient fields, *Proceedings of The International Symposium on Underwater Technology, UT 2007 - International Workshop on Scientific Use of Submarine Cables and Related Technologies 2007*, Institute of Industrial Science, University of Tokyo, Tokyo, Japan., pp 512-519.

[8] Healey, A. J., Artificial Potential Functions, In Roberts & Sutton, (Ed.) *Guidance Laws, Obstacle Avoidance, Artificial Potential Functions*, 3, part of IEEE Control Series 69 (Institute of Electrical and Electronic Engineers 2006).

[9] Healey, A.J., *et al.*, Collaborative Unmanned Systems for Maritime and Port Security Operations, *Proceedings of the 7th IFAC Conference on Control Applications in Marine Systems*, Center for Underwater Systems and Technologies, Zagreb, Croatia, 2007, on CD.

[10] Arnold V. I., Kozlov V. V. & Neishtadt, A. I., *Mathematical aspects of classical and celestial mechanics* (Springer-Verlag, 1997).

[11] Fadenza, P. V. and P. U. Lima, Non-holonomic robot formation with obstacle compliant geometry, *Proceedings of the 6th IFAC Symposium on Intelligent and Autonomous Vehicles*, Devy, M. (ed.), CNRS Laboratoire d'Architecture et d'Analyse des Systemes, Toulouse, France, 2007, on CD.

[1] The Ministry of Science, Education and Sports of the Republic of Croatia.

[2] a non-for-profit non-government civil organization of underwater system engineers and scientists registered in Zagreb, Croatia.